AIHAJ 62:563–572 (2001) Ms. #299

Capture Envelopes of Rectangular Hoods in Cross Drafts

AUTHORS
Rong Fung Huang[a]
Soon Yih Sir[a]
Yu-Kang Chen[b]
Wen-Yu Yeh[c]
Chun-Wann Chen[c]
Chih-Chieh Chen[d]

[a]Department of Mechanical Engineering, National Taiwan University of Science and Technology, 43 Keelung Road, Section 4, Taipei, Taiwan; E-mail: rfhuang@mail.ntust.edu.tw;
[b]Department of Occupational Safety and Hygiene, Chang Jung Christian University, Kway Jen, Taiwan;
[c]Institute of Occupational Safety and Health, Council of Labor Affairs, 132 Min-Sheng E. Rd., Taipei, Taiwan;
[d]Institute of Occupational Medicine and Industrial Hygiene, National Taiwan University, 1 Jen-Ai Rd., Sec. 1, Taipei, Taiwan

This research was supported by the Institute of Occupational Safety and Health, Council of Labor Affairs of Taiwan.

The suction fields of the rectangular hoods of various aspect ratios varying from 0.1 to 10 that are subject to the influence of cross drafts were experimentally studied in an apparatus consisting of a hood model/wind tunnel assembly. The velocity field on the symmetry plane was measured with a two-component laser Doppler anemometer. Being under the influence of cross draft, the suction field presents a characteristic capture envelope, which is described by a dividing streamline. The characteristics of the capture envelope were found to be determined by the cross-draft to hood-suction velocity ratio R and the hood-opening aspect ratio AR. The flow characteristics of the hoods with aspect ratios less than unity were dramatically different from those with aspect ratios greater than one. If areas of the hood openings had the same values, the hydraulic-diameter normalized characteristic length scales of the capture zone of the square hood were as same as those of the circular hood. When the diameter of a circular hood was equal to the width of a square hood, the physical dimensions of the capture zones created by these two hoods coincided with each other.

Keywords: capture envelope, cross draft, hood, limiting trajectory

A properly designed local exhaust ventilation system is an effective way to control airborne contaminants in the workplace. Contaminant transportation and local ventilation efficiency are mainly dependent on the interactions of several factors, for instance, (1) the flow generated by the exhaust opening; (2) the properties of the contaminants; (3) the flow generated by the contaminating source; (4) any blockages (e.g., workers, tools, devices, etc.) in the suction flow field; (5) any perturbing cross drafts and other disruptive air movements; and (6) turbulent dispersion in the flow field.

The first four factors contribute to the conventional concept of *capture velocity,* which is applied to the removal of airborne contaminants with local exhaust ventilation. The capture velocity is defined as "the velocity at any point in front of the hood necessary to overcome opposing air currents and capture the contaminated air by causing it to flow into the hood."[1] The velocities along the centerline axis of free-standing symmetric inlets are the most convenient index to characterize the capture velocity. Besides, describing the velocities along the centerline axis is a relatively simple matter compared with the whole velocity field of the inflowing air stream. Dalla Valle,[2,3] Dalla Valle and Hatch,[4] and Silverman[5–7] have presented the oldest centerline velocity data for circular, rectangular, and narrow slot hoods. Garrison[8] and Braconnier[9] have provided a wide review on the centerline velocity gradients for plain and flanged local exhaust inlets. Garrison[10,11] also presented graphical design concepts and empirical design equations for the calculations of centerline velocities.

The perturbing cross-draft is perhaps the most complex and variable of the influential factors.[12] Such airflows may be induced from various sources such as open windows, doors, cooling fans, moving objects, walking persons, air-conditioning currents, and so forth. In many cases, entirely random, unsteady, gusting, turbulent, or cyclonic complex drafts are unavoidable. The capture zone of a circular hood in the presence of a uniform cross draft presents an envelope with a contour similar to a half Rankine body-of-revolution[13,14] instead of a bell shape. A Rankine body-of-revolution is a flow structure formed from the linear-superposition of a sink and a rectilinear flow. The suction opening of the hood is enclosed in the envelope so that all streamlines within the envelope go to the opening. Those outside the envelope evolve to the

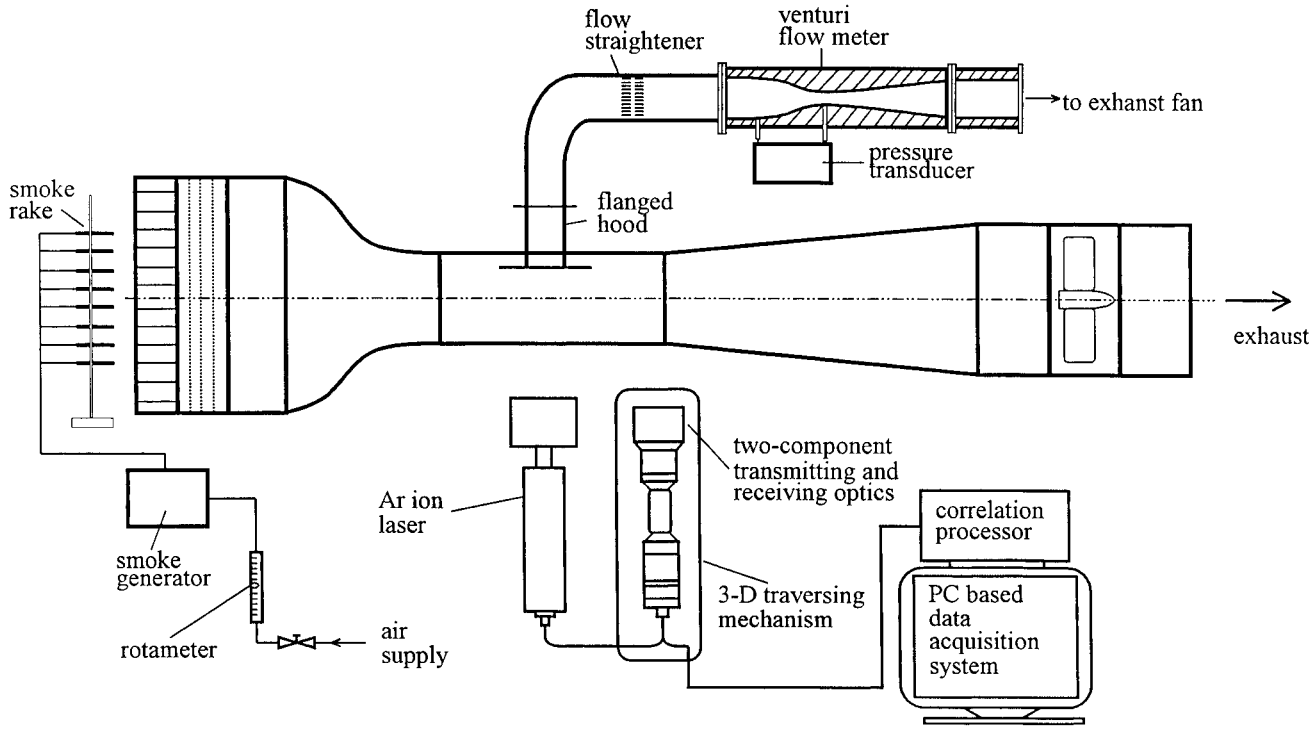

FIGURE 1. Experimental setup

Nomenclature

A	area of hood opening ($=\pi D^2/4$)
AR	aspect ratio ($=L_z/L_x$)
D	diameter of circular hood opening, 10 cm
D_h	hydraulic diameter of rectangular hood ($=4A/P$)
L_{eff}	effective length denoting two-dimensionality of capture envelope
L_x	length of rectangular hood opening
L_z	width of rectangular hood opening
Q_s	volumetric suction rate of exhaust hood
P	peripheral length of rectangular hood ($=2(L_x+L_z)$)
R	cross draft to hood suction velocity ratio ($=V_c/V_s$)
Re_c	Reynolds number of cross draft based on hydraulic diameter of hood opening ($=V_cD_h/\nu$)
Re_s	Reynolds number of suction flow based on hydraulic diameter of hood opening ($=V_sD_h/\nu$)
V_c	velocity of cross draft
V_s	averaged suction velocity of exhaust hood ($= Q_s/A$)
W	width of flange
x	coordinate along direction of cross draft, originated at center of hood opening
y	coordinate along hood center line, originated at center of hood opening
z	coordinate normal to x and y coordinates, originated at center of hood opening
ν	kinematic viscosity of air
ξ	distance in $-$y direction from x axis to lower limit of capture envelope
ζ	distance in x direction from center of hood opening to stagnation point of dividing streamline
η	distance in $-$y direction from origin to intersection of hood center line and dividing streamline

downstream area. The contaminant outside the envelope tends to escape from capture at the exhaust opening if the dispersion effect is ignored. In such a situation the contaminant sources originally placed under the hood may go beyond the effective capture envelope. This would lead to a breakdown of the hood performance. Under these conditions, the concept of "capture velocity" becomes less effective and "capture efficiency" is a more meaningful index of hood performance,[12,15–19] and therefore is a more useful concept in ventilation design.

The capture efficiency[15] is defined as the ratio of the capture rate of the hood to the contaminant generation rate. Flynn and Ellenbecker[12] measured the capture efficiency of sulfur hexafluoride (SF_6) tracer gas released from a fritted ceramic small sphere under a circular hood that was subject to a cross draft. They proposed a formula for calculating the critical centerline distance at which the capture efficiency is 50%:

$$\left[\frac{\text{centerline distance}}{\text{hood diameter}}\right]_{\text{capture efficiency}=50\%} = 0.372\left[\frac{\text{cross draft velocity}}{\text{suction velocity of hood}}\right]^{-0.595} \quad (1)$$

However, obtaining the capture efficiency by experiments is usually a tedious process. Huang et al.[20] conducted experiments on the flow field of a finite-opening circular hood that was subject to the influence of a cross draft. Both the phenomenological and quantitative results were obtained. Streak patterns obtained from the smoke-trajectory flow visualization method were employed to clarify the variations of flow field. The streamline patterns obtained from the measured velocity data signify the capture envelope characteristics. Semiempirical formulae based on the classical potential theory[13,14] that a point source is superimposed by a rectilinear

TABLE I. Aspect Ratio and Dimensions of Hood Opening

AR (=L_z/L_x)	L_z (cm)	L_x (cm)	D_h (cm)
00.1	02.80	28.00	5.10
00.4	05.61	14.00	8.01
01.0	08.86	08.86	8.86
05.0	19.80	03.97	6.61
10.0	28.00	02.80	5.10

flow were derived to assist in finding the primary parameters of hood design and the proper locations of contaminant sources. The authors also verified that both their dividing streamline method and Flynn and Ellenbecker's aerosol sampling technique[12] are eligible for the evaluation of the characteristic length scales of hood performance. The flow field, particularly the capture envelope, thus becomes indicative of the capture performance.

The slot, square, and rectangular hoods have been widely used in many applications. However, the characteristics of the capture envelopes in the flow field of a rectangular suction hood that is subject to a cross draft have not been intensively studied, partly because of the complexities in the hood geometry. Experimental results on the flow characteristics of the capture zone were limited. In this article the flow characteristics of flanged slot, square, and rectangular hoods of various aspect ratios at various suction-to-cross draft velocity ratios were probed. The velocities were measured with a two-component laser Doppler anemometer. The streamline patterns were obtained from the measured velocity data. The boundary of the effective capture envelope was described by a dividing streamline that attained a stagnation point on the flange. The capture envelopes were finally characterized by the cross draft-to-hood suction velocity ratio R and the hood-opening aspect ratio AR.

EXPERIMENTAL ARRANGEMENTS

Figure 1 shows the experimental apparatus. The system included a hood model, a wind tunnel, peripheral devices, and instruments for measurements. The cross draft was supplied by an open-loop wind tunnel, which was described by Huang et al.[20] For the sake of convenience and completeness, it is briefly summarized here. The test section, which was made of transparent acrylic plates, has a cross section of 50×50 cm and a length of 120 cm. The velocity range of stable operation was between 0.05 and 20.0 m/sec. The turbulence intensity was less than 0.40% when the wind velocity V_c was greater than 1.2 m/sec. The turbulence intensity increased with the decrease of wind velocity when V_c was less than 1.2 m/sec; for example, the turbulence intensity was 0.85% at V_c = 0.4 m/sec. A hot-wire anemometer calibrated by a laser Doppler velocimeter was used to measure and monitor the free-stream velocity of the cross draft. The accuracy of the free-stream velocity measurement was about 0.5% of the reading.

Five hood models made of acrylic plates were used in this study. The area of each hood opening was equivalent to the area of a circular opening with a diameter D = 10.0 cm. However, the aspect ratios AR (width-to-length ratio) varied. They were 0.1, 0.4, 1, 5, and 10, covering the range of slot, square, and rectangular hoods. The dimensions and hydraulic diameters of these hoods are listed in Table I. A sharp-edged acrylic square flat plate was attached on the plane of the hood opening to serve as the flange. The width and thickness of the flange were 40 cm and 0.4 cm, respectively. The hood model was installed at the center of

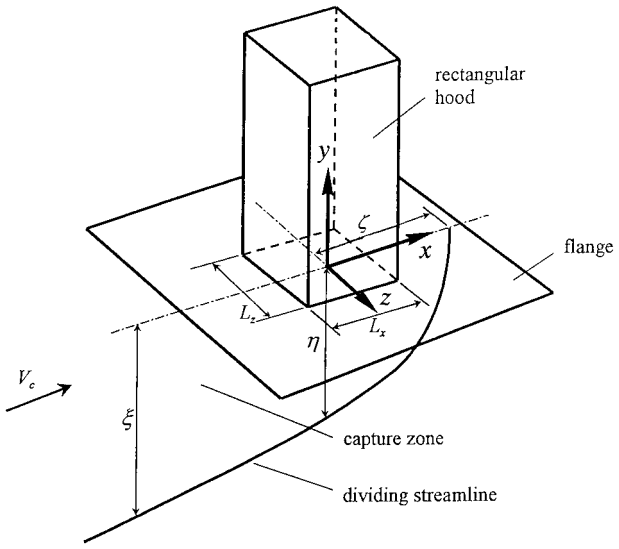

FIGURE 2. Coordinate system and symbols denoting characteristic length scales of capture zone

the test section and protruded perpendicularly through the ceiling plate 4 cm down into the test section. The maximum thickness of the wall boundary-layer in the current experimental range was estimated to be about 1.5 cm at the center of the test section so that no significant distortion of the flow field into the hood was caused by the effects of the wind tunnel walls. Positions are described in terms of a Cartesian coordinate system (x, y, z), as shown in Figure 2. The characteristic length scales ξ, ζ, and η are also shown in Figure 2. Suction of the hood was provided via a centrifugal fan. The suction flow rate was measured by a venturi flow meter along with an electronic pressure transducer. The accuracy of the suction flow rate measurement was less than 2% of the reading.

The experimental range of the suction Reynolds number Re_s was from 1.80×10^4 to 6.0×10^4. The cross-draft Reynolds number Re_c was between 0.14×10^4 and 2.36×10^4. The cross draft-to-suction velocity ratio R covered from 0.075 to 0.752.

Laser Doppler Velocimeter (LDV)

The velocity field was measured with a two-component laser Doppler velocimeter (Fiber Flow Optics 9060×0411 and FVA Enhanced Signal Correlator 58N40, Dantec Measurement Technology, Skovlunde, Denmark). A 5 W argon-ion laser was used as the light source. The blue and green laser beams were separated, split, and focused through an optical system. The dimensions of measuring volumes of the green and blue components were 0.075 × 0.075 × 0.680 mm and 0.071 × 0.071 × 0.645 mm, respectively. The fringe separations of the green and blue components were 2.34 μm and 2.22 μm, respectively. The system was configured for backward scattering. A Bragg cell and two electronic frequency shifters were included in the system. Two correlation processors were used to capture the frequency of the signals. The digital outputs of the counter processors were fed into a data acquisition system. Each velocity data record consisted of 300 samples, about 1.5 sec long. Uncertainty of the velocity measurements is estimated to be less than ±0.5% of the reading.

Mineral oil mist was continuously seeded through a homemade smoke generator into the test section via a tube rake to scatter the

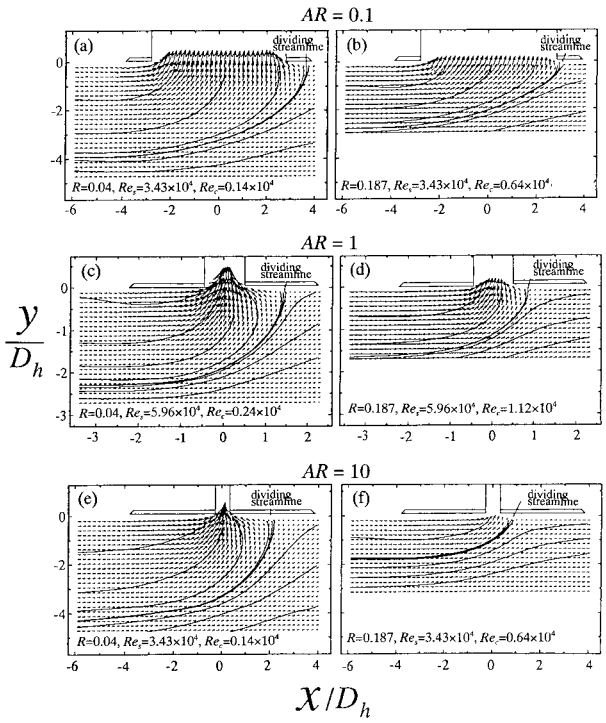

FIGURE 3. Velocity vectors and streamlines measured by LDV. (a, b) AR = 0.1; (c, d) AR = 1; (e, f) AR = 10.

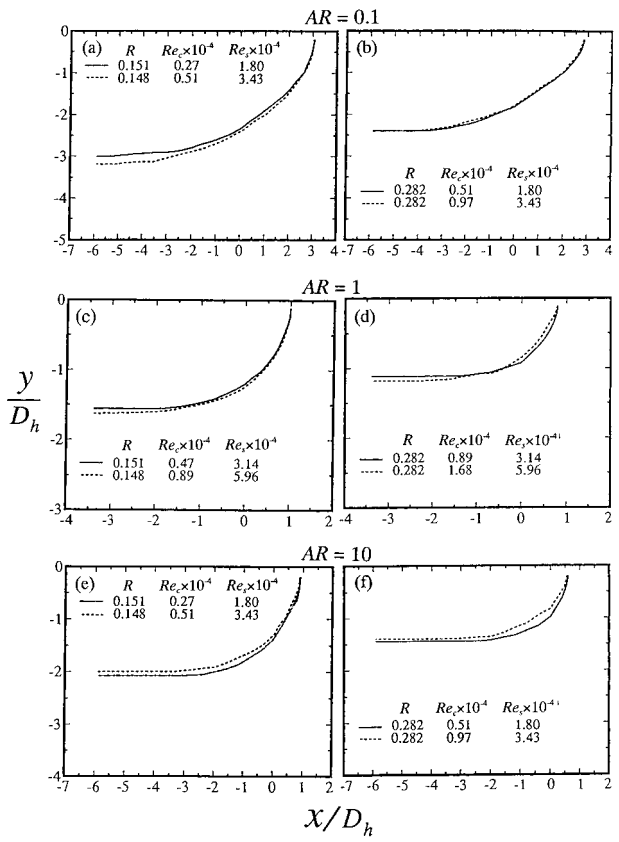

FIGURE 4. Comparisons of dividing streamlines at similar velocity ratios. (a, b) AR = 0.1; (c, d) AR = 1; (e, f) AR = 10.

laser light. The diameter of the oil-mist particles, measured by a Malvern 2600C particle analyzer, was 1.7 ± 0.2 μm. The density was 0.821 g/mL. Ignoring the effect of turbulent diffusion, the relaxation time constant was estimated to be less than 7.7×10^{-5} sec, and the Stokes number was on the order of 10^{-6} within the range of experiment. Therefore, the seeding particles could properly follow the flow fluctuations at least up to 10 kHz.[21]

RESULTS AND DISCUSSION

Capture Envelope and Dividing Streamline

To obtain quantitative and detailed information of the flow field, the two-component laser Doppler velocimeter (LDV) was used to measure the velocity distributions on the symmetry plane of the hood opening. About 22 different R values of flow fields were measured for each hood. Different pairs of Re_s and Re_c may provide similar values of R so that comparisons based on similar R are possible.

Figure 3 shows the normalized velocity vector fields and streamline patterns for different aspect ratios. For all aspect ratios, the velocity vectors near the hood opening possessed larger x components. Far away from the opening, the y components were large. A streamline denoted by "dividing streamline" evolved far from upstream, rose up, and hit perpendicularly to the flange to form a stagnation point. In the upper left part of the flow field enclosed in the dividing streamline, which is called the capture envelope, all the streamlines evolving from upstream went to the hood opening. Theoretically, all the contaminants inside the capture envelope should follow the flow and be attracted into the hood opening if the dispersion effect is ignored.

For the same aspect ratio AR, the capture envelope shrinks with the increase of velocity ratio R. For instance, for AR = 0.1, the normalized lower limit and stagnation point of the dividing streamline in Figure 3(a) for R = 0.04 were $y/D_h \approx -4$ and $x/D_h \approx 3.7$, respectively. However, they reduced to $y/D_h \approx -2.8$ and $x/D_h \approx 3$ in Figure 3(b), respectively, as R increased to 0.187. The same situations occur in Figures 3(c) and (d) for AR = 1, as well as in Figures 3(e) and (f) for AR = 10. By comparing Figures 3(a), (c), and (e), or Figures 3(b), (d) and (f), it can be seen that the square hood (AR = 1) had the smallest normalized capture zone. By comparing Figures 3(a) and (b) for AR = 0.1 with Figures 3(e) and (f) for AR = 10, it can be seen that the normalized capture zones of AR = 0.1 were larger than those of AR = 10, even though their hydraulic diameters had the same value (5.10).

Figure 4 shows the normalized dividing streamlines at R ≈ 0.15 (Figures 4[a], [c], and [e]) and R ≈ 0.28 (Figures 4[b], [d], and [f]) for different ARs. For each AR, the dividing streamlines at similar values of R almost coincide with each other, no matter what the Reynolds numbers of cross draft and suction are. When comparisons are made among Figures 4(a), (c), and (e) at R ≈ 0.15, the normalized dividing streamlines for AR = 0.1, 1, and 10 are not coincident. The same results are found at R ≈ 0.28, as shown in Figures 4(b), (d), and (f). In either case, the capture zone for AR = 1 was the smallest.

Square and Circular Openings

The extent of the capture zone can be characterized by three characteristic length scales, η, ξ, and ζ. The contaminant source on the center line can be installed within the range of the distance η.

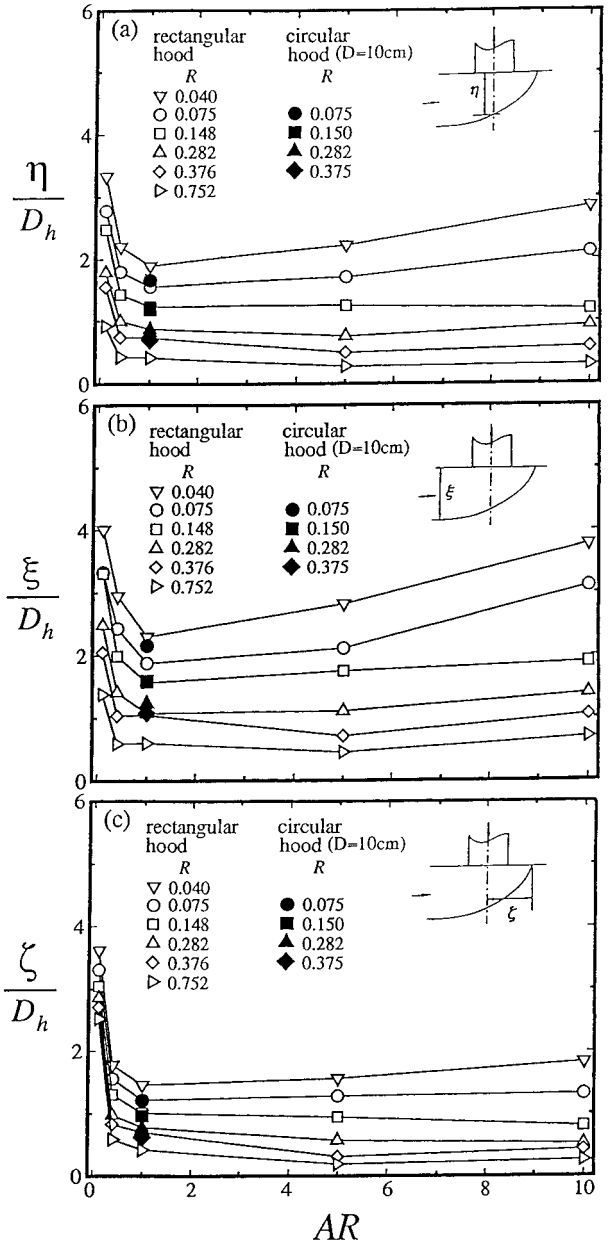

FIGURE 5. Variations of normalized characteristic length scales of capture zone with aspect ratio

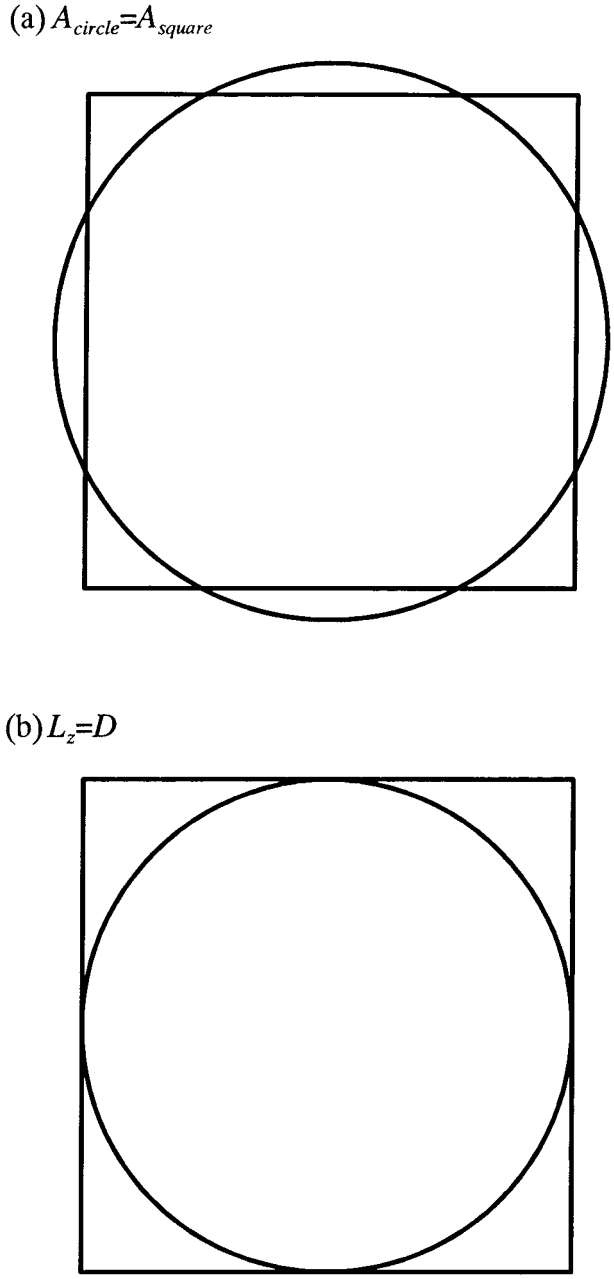

FIGURE 6. Circular and square openings. (a) Same areas lead to same hydraulic-diameter normalized characteristic length scales of capture zone; (b) square inscribed in circle, L_z = D, leads to same physical dimensions of capture zone.

The distance ξ offers the estimation of the off-center-line location for the contaminant source. The length ζ enables the designer to calculate minimum required flange size under designated R and AR. Figures 5(a), (b), and (c) show the variations of the normalized characteristic lengths η/D_h, ξ/D_h, and ζ/D_h, respectively. At all velocity ratios, the normalized characteristic lengths decrease fast with the increase of aspect ratio when AR < 1. η/D_h, ξ/D_h, and ζ/D_h attain minimum values at AR = 1, then increase inappreciably with the increase of aspect ratio when AR > 1. Especially, as R is greater than about 0.14, the normalized characteristic length scales remain almost unchanged. What is notable is that the normalized characteristic length scales of the circular hood (data adopted from Huang et al.[20] are marked with the filled symbols) almost coincide with those of the square hood.

This result justifies the use of the normalizing parameter D_h. For the circular and square hoods with the same opening area at the same R, their normalized dividing streamlines (or normalized extents of capture zones) on the symmetry plane coincide with each other. However, if the physical dimensions are considered at the same velocity ratio R, the capture zone generated by the circular hood would be larger than that by the equal-area square hood because the hydraulic diameter D_h of the circular hood is larger than that of the square hood. For instance, as shown in Figure 6(a), the square opening had a physical width of 8.86 cm and a hydraulic diameter D_h = 8.86 cm. Both the physical and hydraulic diameters of the equal-area circular opening were 10 cm.

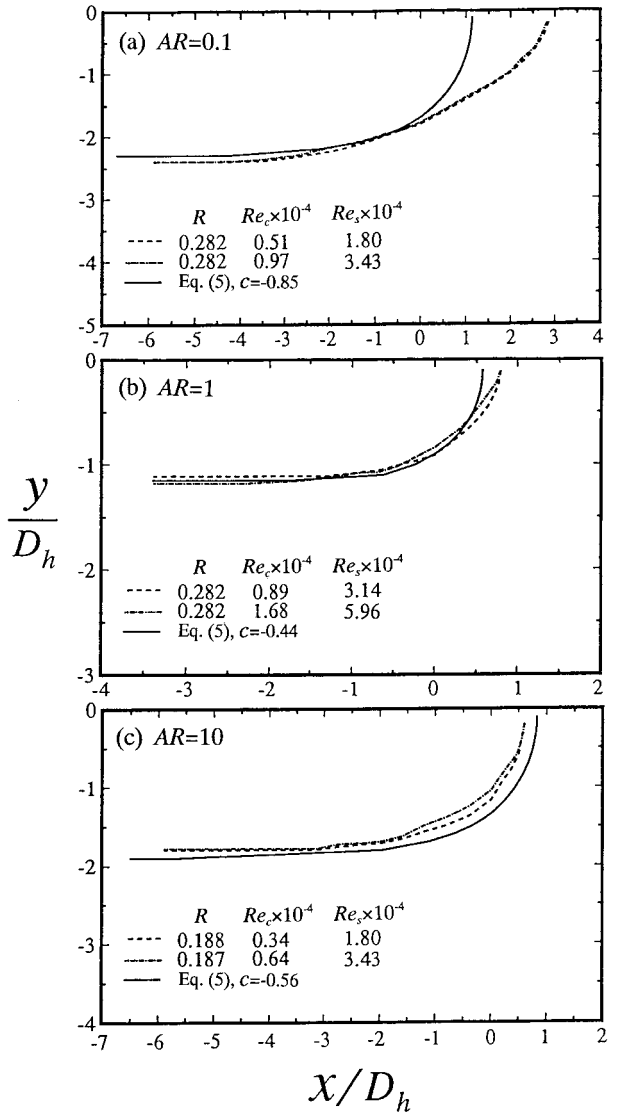

FIGURE 7. Comparisons of dividing streamlines between experimental results and correlation using finite-opening potential flow theory

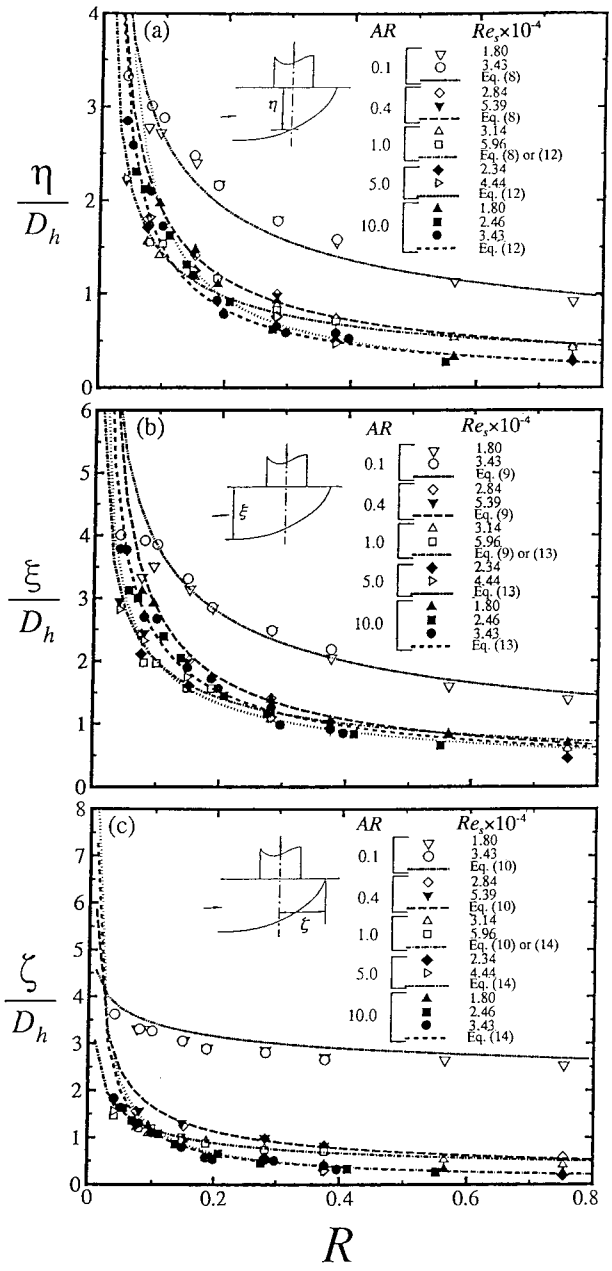

FIGURE 8. Comparisons of normalized characteristic length scales of capture zone with recommended correlation

Both the square and circular openings' D_h-normalized characteristic lengths on the symmetry plane had the same values, as shown in Figure 5. However, the physical characteristic lengths of the capture envelope of the equal-area circular hood were about 13% larger than those of the square hood. The general relationship may be derived by the following simple analysis. The hydraulic diameter of the circular hood was $(D_h)_{circular} = 4A/P = 4A/\pi D$. The hydraulic diameter of the square hood was $(D_h)_{square} = 4A/P = 4A/4L_z$.[22] Because the areas had the same value, the hydraulic diameter ratio between the circular and square hoods was

$$\frac{(D_h)_{circular}}{(D_h)_{square}} = \frac{\frac{4A}{\pi D}}{\frac{4A}{4L_z}} = \frac{4L_z}{\pi D} \qquad (2)$$

Because the normalized characteristic lengths of the circular hood were the same as those of the square hood, that is, (physical dimensions of capture zone)$_{circular}$/$(D_h)_{circular}$ = (physical dimensions of capture zone)$_{square}$/$(D_h)_{square}$, the ratio between the physical sizes of the capture zones of the circular and square hoods read

$$\frac{(\eta, \xi, \zeta)_{circular}}{(\eta, \xi, \zeta)_{square}} = \frac{(D_h)_{circular}}{(D_h)_{square}} = \frac{4L_z}{\pi D} \qquad (3)$$

for hoods with the same opening areas. In other words, to obtain the same physical size of the capture zone on the symmetry plane, the required area of the circular hood was smaller than that of the square hood, viz.,

$$\frac{A_{circular}}{A_{square}} = \frac{\pi D}{4L_z} \qquad (4)$$

for the same sizes of capture zone on symmetry plane. Because $A_{circular}/A_{square} = (\pi D^2/4)/L_z^2 = \pi D^2/(4L_z^2)$, the ratio of the diameter of the circular opening and the width of the square opening must be

$$\frac{D}{L_z} = 1 \tag{5}$$

When $D = L_z$, the circular opening was inscribed in the square opening, as shown in Figure 6(b). The area ratio of the circular opening inscribed in the square opening with $D = L_z$ was $\pi D/4L_z$. Conroy et al.[18] employed an inscribed ellipse and an equal-area ellipse to simulate a rectangular hood. Four different models of potential flow theory were applied to calculate the flow fields. They concluded that the inscribed ellipse was a better predictor of performance than the equal-area ellipse. Their conclusion supports the current results and discussion. At the same suction rate, the inscribed circular opening had a larger face velocity than did the square opening. This factor would favor the increase of the capture zone of the circular hood. However, the corners of the square opening increased the two-dimensionality; therefore, the resistance to the cross-draft was increased. This factor favors the size enlargement of the capture zone of the square hood. The combination of these two effects led to the present results.

Correlation of Dividing Streamlines and Characteristic Length Scales

According to the models proposed by Huang et al.,[20] the dividing streamline and characteristic length scales of the capture envelope that is subject to a cross draft can be represented by forms similar to the results of the classical potential theory[13,14] that a point sink with a strength Q_s superimposed by a rectilinear flow with a velocity V_c. The point sink strength is modeled by the suction flow rate of the hood. The nondimensional equations of the dividing streamline and characteristic lengths turn out to be the functions of $R^{-0.5}$ as in the classical potential flow theory of point-sink-plus-rectilinear-flow. However, in a practical situation, the coefficients and exponent of R should be slightly modified owing to the following reasons: (1) the hood has a finite suction opening instead of a point sink, (2) the fluid is not inviscid even though the viscosity is small, and (3) the dispersion effect is not completely negligible. For the circular hood, the correlation is[20]

Dividing streamline:

$$\frac{x}{D} = \frac{c}{\sqrt{R}}\sqrt{\left(1 - \frac{\frac{y}{D}}{\sqrt{\left(\frac{x}{D}\right)^2 + \left(\frac{y}{D}\right)^2}}\right)} \tag{6}$$

where $c = -0.44$.

Characteristic lengths:

$$\frac{\delta}{D} = \frac{\chi}{R^m} \tag{7}$$

where $\chi = 0.4073$, $m = 0.5533$ for $\delta = \eta$; $\chi = 0.6216$, $m = 0.4924$ for $\delta = \xi$; $\chi = 0.4285$, $m = 0.4135$ for $\delta = \zeta$.

If the function in Equation 6 is employed to correlate the dividing streamlines of the rectangular hoods, the diameter D must be replaced by D_h and the constant c be varying for each aspect ratio. The best fit becomes: $c = -0.85$ for $AR = 0.1$; $c = -0.44$ for $AR = 1$; and $c = -0.559$ for $AR = 10$. Figure 7 shows the examples of the fitted results. The correlation deviates significantly from the measurements around the region near the stagnation point, particularly at low aspect ratios. Obviously, the modeling of the point sink strength by the hood suction is inappropriate for the rectangular openings so that the correlation applying the classical potential flow theory deviates significantly from the measurements.

In the present case, the velocity ratio R is not the sole dominant parameter. The geometric parameter AR must be taken into account, as has been shown in Figures 3–5. In Figure 5 the variation of the normalized geometry of the dividing streamlines with the aspect ratio is not a monotonically increasing or decreasing function. It would be impractical to correlate the characteristic length scales to a satisfactory precision with just a single set of equations for the whole range of the aspect ratio. Dividing the correlation range into $AR \le 1$ and $AR \ge 1$, the authors provide the following correlation equations for practical uses. Computer programs for solving the following equations are available on request from the authors.

(A) $AR \le 1$

Dividing streamline:

$$\begin{aligned}\frac{y}{D_h} = {} & \{[(29.05 \times AR^2 - 24.64 \times AR + 2.77) \times R^2] \\ & + [(-8.69 \times AR^2 + 7.46 \times AR - 0.97) \times R] \\ & + (-0.43 \times AR^2 - 0.19 \times AR + 0.05)\} \times \left\{\left(\frac{x}{D_h}\right)^3\right\} \\ & + \{[(23.52 \times AR^2 - 22.19 \times AR + 0.89) \times R^2] \\ & + [(-7.07 \times AR^2 + 6.98 \times AR - 0.25) \times R] \\ & + (-0.09 \times AR^2 + 0.49 \times AR - 0.01)\} \times \left\{\left(\frac{x}{D_h}\right)^2\right\} \\ & + \{[(-26.06 \times AR^2 + 24.04 \times AR - 6.43) \times R^2] \\ & + [(7.53 \times AR^2 - 7.09 \times AR + 2.58) \times R] \\ & + (-1.11 \times AR^2 + 1.32 \times AR - 0.01)\} \times \left(\frac{x}{D_h}\right) \\ & + \{[(-40.11 \times AR^2 + 39.19 \times AR - 10.81) \times R^2] \\ & + [(-4.46 \times AR^2 + 5.78 \times AR + 6.16) \times R] \\ & + (-2.31 \times AR^2 + 3.68 \times AR - 3.47)\}\end{aligned} \tag{8}$$

Characteristic lengths:

$$\frac{\eta}{D_h} = \frac{0.3444 \times (5.298 \times AR^2 - 7.367 \times AR + 3.221)}{R^{0.5\times(-1.949\times AR^2+2.302\times AR+0.754)}} \tag{9}$$

$$\frac{\xi}{D_h} = \frac{0.5143 \times (5.596 \times AR^2 - 7.59 \times AR + 3.237)}{R^{0.5\times(-2.477\times AR^2+2.785\times AR+0.677)}} \tag{10}$$

$$\frac{\zeta}{D_h} = \frac{0.2667 \times (29.353 \times AR^2 - 41.166 \times AR + 13.527)}{R^{0.5\times(-3.651\times AR^2+4.661\times AR-0.182)}} \tag{11}$$

(B) $AR \ge 1$

Dividing streamline:

$$\frac{y}{D_h} = \left(\frac{-0.3536 \times (0.005 \times AR^2 - 0.018 \times AR + 1.228)}{\sqrt{R}}\right) \times \sqrt{\left(1 - \frac{\frac{x}{D_h}}{\sqrt{\left(\frac{x}{D_h}\right)^2 + \left(\frac{y}{D_h}\right)^2}}\right)} \tag{12}$$

Characteristic lengths:

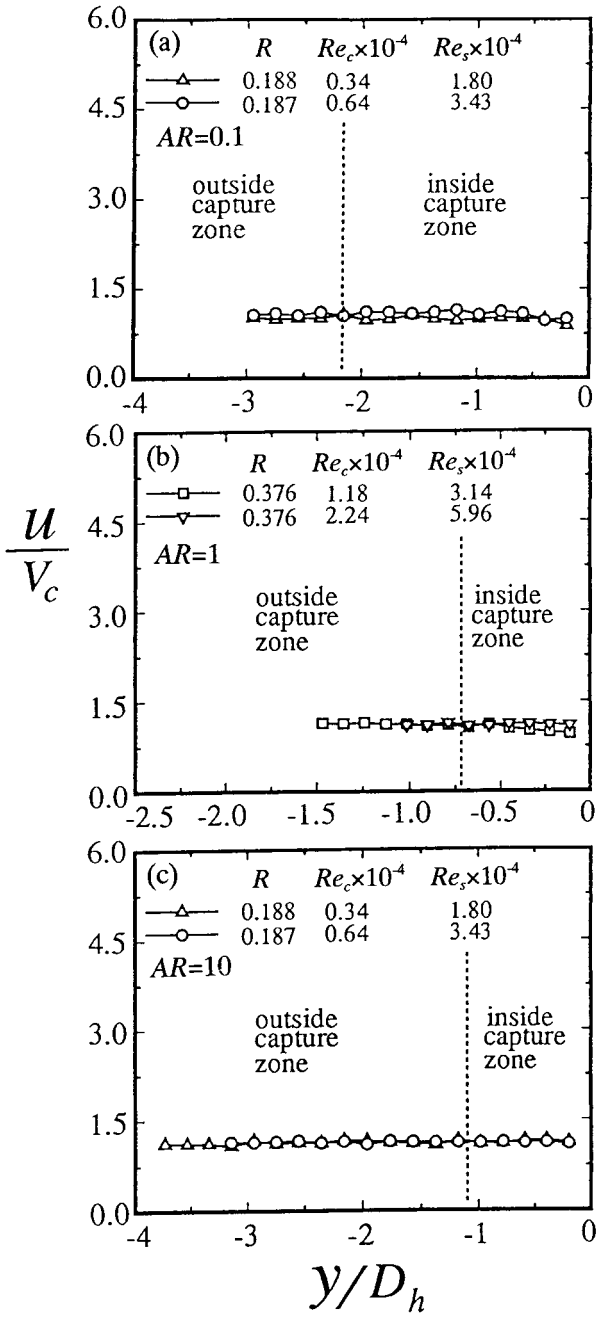

FIGURE 9. Distribution of u/V_c along central axis

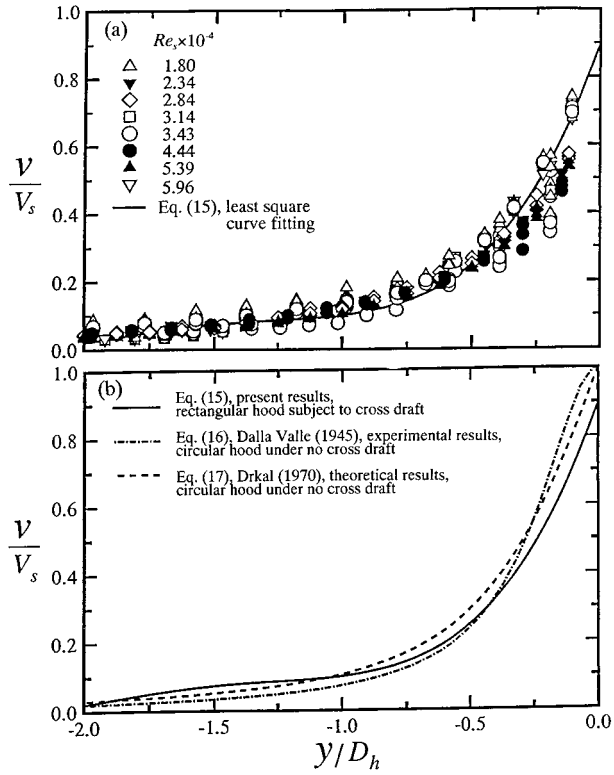

FIGURE 10. Distribution of v/V_s along central axis. (a) Correlation, (b) comparison with previous results without cross draft

$$\frac{\eta}{D_h} = \frac{0.3444 \times (0.016 \times AR^2 - 0.234 \times AR + 1.37)}{R^{0.5\times(-0.027\times AR^2+0.359\times AR+0.775)}} \quad (13)$$

$$\frac{\xi}{D_h} = \frac{0.5143 \times (0.008 \times AR^2 - 0.106 \times AR + 1.342)}{R^{0.5\times(-0.003\times AR^2+0.061\times AR+0.926)}} \quad (14)$$

$$\frac{\zeta}{D_h} = \frac{0.2667 \times (0.029 \times AR^2 - 0.436 \times AR + 2.121)}{R^{0.5\times(-0.025\times AR^2+0.359\times AR+0.492)}} \quad (15)$$

The correlation Equations 8 and 12 for the dividing streamlines fit the experimental results in a maximum deviation under 12%, which is generally acceptable for the purpose of hood design. In the area under the hood opening, that is, $-1 < x/D_h < 1$, the deviation is less than 6%. Because the location and movement of the contaminant sources are usually limited within the projection of the hood opening, the error induced by the deviation of fitting is insignificant.

Figure 8 shows the experimental data and the fitting curves of correlation Equations 9–11 and 13–15. The application guidelines of the correlation equations for the hood design and contaminant positioning were provided by Huang et al.[20] For all aspect ratios, the normalized characteristic lengths decrease drastically with the increase of the velocity for $R < 0.2$. For $R > 0.2$, the decrease

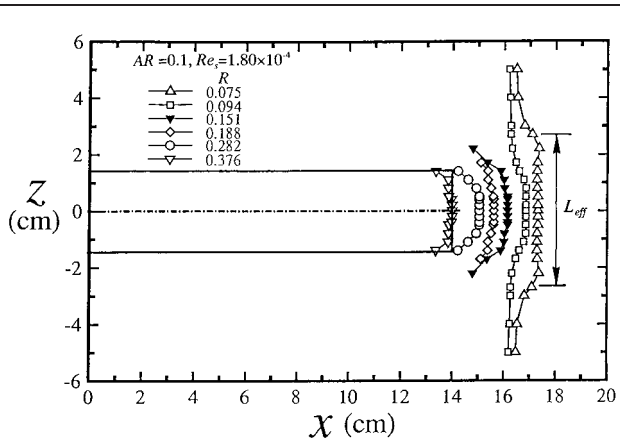

FIGURE 11. Variation of stagnation points in *z*-direction

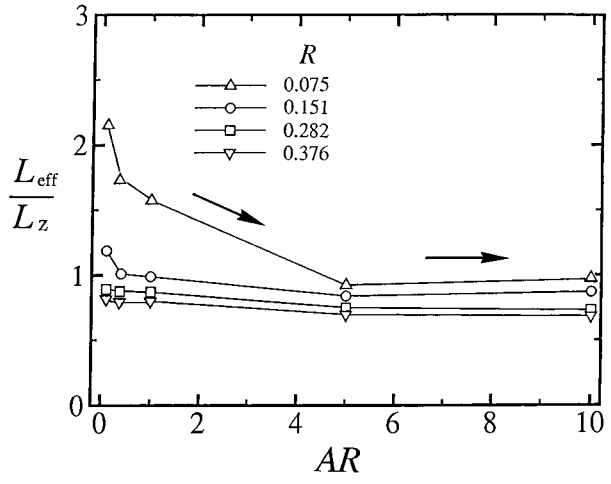

FIGURE 12. Quantification index of two-dimensionality using L_{eff}/L_z

rate becomes inappreciably low. In other words, if the cross-draft velocity is lower than one-fifth of the suction velocity, the effect of the cross draft on the reduction of the capture zone is significant. As the cross-draft velocity increases to values higher than one-fifth of the suction velocity, the effect on the reduction of the capture zone attains almost saturation.

Velocity Along Central Axis

The distributions of the normalized u velocity component, u/V_c, along the central axis are shown in Figure 9. For all AR and R, u/V_c remains almost a constant of about 1.15 along the central line, either inside or outside the capture zone. From the point of view of potential flow theory, the rule of superposition demands $u/V_c = 1$ along the central axis. However, in reality, the suction flow does cause a little influence on the lateral velocity component along the central axis.

The distributions of the normalized v velocity component, v/V_s, along the central axis are shown in Figure 10(a). The data do not scatter widely and can be fitted with the least square method to obtain the following equation:

$$\frac{v}{V_s} = 0.15 \times \left(\frac{y}{D_h}\right)^4 + 0.96 \times \left(\frac{y}{D_h}\right)^3 + 2.17 \times \left(\frac{y}{D_h}\right)^2 + 2.16 \times \frac{y}{D_h} + 0.9 \quad \textbf{(16)}$$

Figure 10(b) shows the comparison of Equation 16 with the famous equations obtained by Dalla Valle[3] and Drkal[23] for the flow field of a suction hood not subject to the influence of the cross draft. Dalla Valle's empirical equation reads

$$\frac{v}{V_s} = \frac{1}{\frac{10}{\pi}\left(\frac{2y}{D_h}\right)^2 + 1} \quad \textbf{(17)}$$

and Drkal's theoretical solution is written

$$\frac{v}{V_s} = 1 + \frac{\frac{2y}{D_h}}{\sqrt{1 + \left(\frac{2y}{D_h}\right)^2}} \quad \textbf{(18)}$$

It is noticeable that near the hood opening in the range $-0.3 < y/D_h < 0$, v/V_s obtained from Equation 16 is a little lower than that calculated from Dalla Valle and Drkal. Because there are relatively few data near $y/D_h = 0$, it may cause the regression to "bend" downward at the end of the curve. However, for $y/D_h < -0.3$, the three curves do not deviate significantly from each other. The normalized v velocity component along the central line is not altered significantly when the suction flow field is subject to the influence of the cross draft.

Two-Dimensionality of Capture Zone

To test the two-dimensionality of the capture zone, the stagnation points off the symmetry plane are detected by laser Doppler velocimeter. Figure 11 shows an example of the results for AR = 0.1. At low velocity ratio R, the stagnation point remains at the same x position in a wide range of z; that is, the two-dimensionality of the capture zone at small R is better than that at large R. To quantify the two-dimensionality, define the effective length L_{eff} as the length in z direction when the x coordinate of the stagnation point decreases 20% from the constant value, as shown in Figure 11. The normalized effective length L_{eff}/L_z, which varies with the aspect ratio R is shown in Figure 12. At small R, the normalized effective length L_{eff}/L_z decreases apparently with the increase of AR when $AR < 1$. When $AR > 1$, L_{eff}/L_z does not decrease significantly with the increase of AR, particularly at large R.

CONCLUSIONS

The characteristics of the capture envelopes in the flow field of a rectangular suction hood that is subject to a cross draft were experimentally studied. The aspect ratios of the suction opening varied from 0.1 to 10. The following conclusions were drawn from the results.

(1) The geometry of the capture envelope of the rectangular hood was decided primarily by the cross draft-to-suction velocity ratio R and the aspect ratio AR of the hood opening. The hydraulic-diameter normalized dividing streamline and characteristic length scales could be correlated with the parameters R and AR. The correlated equations could be applied to the positioning of the contaminant source when the rectangular hood was subject to the influence of a steady, uniform cross draft.

(2) The classical potential theory of the point-sink-plus-rectilinear-flow was not proper to model the flow characteristics of the rectangular hood, although it was appropriate when applied to the circular hood.

(3) If the opening areas of the circular and square hoods were the same, the hydraulic-diameter normalized characteristic length scales on the symmetry plane of these two hoods would be the same. However, the ratio of the physical dimensions of the circular to square hood was $4L_z/\pi D$. To obtain the same physical size of the capture zone on the symmetry plane, the required area of the square hood should be larger than that of the circular hood. In this situation, the circular opening was inscribed in the square opening and followed the equality $D = L_z$.

(4) The appearances of the capture zones varied with the aspect ratio. When $AR < 1$, the normalized length scales of the capture zone decreased drastically with the increase of AR. While in the range of $AR > 1$, the normalized length scales of the capture zone increased inappreciably with the increase of AR.

REFERENCES

1. **American Conference of Governmental Industrial Hygienists:** *Industrial Ventilation—A Manual of Recommended Practice,* 19th ed. Lansing, Mich.: American Conference of Governmental Industrial Hygienists, 1986.
2. **Dalla Valle, J.M.:** *Studies in the Design of Local Exhaust Hoods,* Sc.D. diss. Harvard University, 1930.
3. **Dalla Valle, J.M.:** *Exhaust Hoods.* New York: Industrial Press, 1945.
4. **Dalla Valle, J.M., and T. Hatch:** Studies in the design of local exhaust hoods. *Trans. ASME 54*:31–37 (1932).
5. **Silverman, L.:** Fundamental factors in the design of lateral exhaust hoods for industrial tanks. *J. Ind. Hyg. Toxicol. 23*:187–266 (1941).
6. **Silverman, L.:** Centerline velocity characteristics of round openings under suction. *J. Ind. Hyg. Toxicol. 24*:259–266 (1942).
7. **Silverman, L.:** *Fundamental Factors In The Design of Exhaust Hoods.* Sc.D. diss., Harvard University, 1943.
8. **Garrison, R.P.:** Centerline velocity gradients for plain and flanged local exhaust inlets. *Am. Ind. Hyg. Assoc. J. 42*:739–746 (1981).
9. **Braconnier, R.:** Bibliographic review of velocity fields in the vicinity of local exhaust hood openings. *Am. Ind. Hyg. Assoc. J. 49*:185–198 (1988).
10. **Garrison, R.P.:** Velocity calculation for local exhaust inlets—graphical design concepts. *Am. Ind. Hyg. Assoc. J. 44*:941–947 (1983).
11. **Garrison, R.P.:** Centerline velocity gradients for plain and flanged local exhaust inlets. *Am. Ind. Hyg. Assoc. J. 44*:937–940 (1983).
12. **Flynn, M.R., and M.J. Ellenbecker:** Capture efficiency of flanged circular local exhaust hoods. *Ann. Occup. Hyg. 30*:497–513 (1986).
13. **Yuan, S.W.:** *Foundations of Fluid Mechanics.* Englewood Cliffs, N.J.: Prentice Hall, 1967.
14. **Currie, I.G.:** *Fundamental Mechanics of Fluids.* New York: McGraw-Hill, 1974.
15. **Ellenbecker, M.J., R.J. Gempel, and W.A. Burgess:** Capture efficiency of local exhaust ventilation systems. *Am. Ind. Hyg. Assoc. J. 44*: 752–755 (1983).
16. **Flynn, M.R., and M.J. Ellenbecker:** The potential flow solution for air flow into a flanged circular hood. *Am. Ind. Hyg. Assoc. J. 46*:318–322 (1985).
17. **Flynn, M.R., and M.J. Ellenbecker:** Empirical validation of theoretical velocity fields into flanged circular hoods. *Am. Ind. Hyg. Assoc. J. 48*:380–389 (1987).
18. **Conroy, L.M., M.J. Ellenbecker, and M.R. Flynn:** Prediction and measurement of velocity into flanged slot hoods. *Am. Ind. Hyg. Assoc. J. 49*:226–234 (1988).
19. **Flynn, M.R., and C. Miller:** Comparison of models for flow through flanged and plan circular hoods. *Ann. Occup. Hyg. 32*:373–384 (1988).
20. **Huang, R.F., J.L. Chen, Y.-K. Chen, C.-C. Chen, W.-Y. Yeh, and C.-W. Chen:** The capture envelope of a flanged circular hood in cross drafts. *Am. Ind. Hyg. Assoc. J. 62*:199–207 (2001).
21. **Flagan, R.C., and J.H. Seinfeld:** *Fundamentals of Air Pollution Engineering.* Englewood Cliffs, N.J.: Prentice Hall, 1988.
22. **Shames, I.H.:** *Mechanics of Fluids.* New York: McGraw-Hill, 1992.
23. **Drkal, F.:** Strömungsverh ältnisse bei runden saug öffnugen mit flansch. *Z. Heiz. Lüft. Klim. Haus. 21*:271–273 (1970).